Journal of Pharmaceutical Sciences 107 (2018) 2251-2258

Contents lists available at ScienceDirect

Journal of Pharmaceutical Sciences

journal homepage: www.jpharmsci.org

Pharmacokinetics, Pharmacodynamics and Drug Transport and Metabolism

Spectral Reflectance Measurement of Evaporating Chemical Films: Initial Results and Application to Skin Permeation

H. Frederick Frasch*, Larry Lee, Ana M. Barbero

Health Effects Laboratory Division, National Institute for Occupational Safety and Health, Morgantown, West Virginia 26508

ARTICLE INFO

Article history:
Received 14 February 2018
Revised 12 April 2018
Accepted 20 April 2018
Available online 27 April 2018

Keywords:
diffusion
in vitro model(s)
mathematical model(s)
passive diffusion
percutaneous
skin
solvent evaporation
transdermal

ABSTRACT

The present study has 2 aims. First, the method of spectral reflectance was used to measure evaporation rates of thin (~25-300 μm) films of neat liquid volatile organic chemicals exposed to a well-regulated wind speed u. Gas-phase evaporation mass transfer coefficient (k_{evap}) measurements of 10 chemicals, 9 of which were measured at similar u, are predicted (slope of log-log data = 1.01; intercept = 0.08; $R^2 = 0.996$) by a previously proposed mass transfer correlation. For one chemical, isoamyl alcohol, the dependence of k_{evap} on $u^{0.52}$ was measured, in support of the predicted exponent value of ½. Second, measured k_{evap} of nicotine was used as an input in analytical models based on diffusion theory to estimate the absorbed fraction (F_{abs}) of a small dose (5 μL/cm^2) applied to human epidermis *in vitro*. The measured F_{abs} was 0.062 ± 0.023. Model-estimated values are 0.066 and 0.115. Spectral reflectance is a precise method of measuring k_{evap} of liquid chemicals, and the data are well described by a simple gas-phase mass transfer coefficient. For nicotine under the single exposure condition measured herein, F_{abs} is well-predicted from a theoretical model that requires knowledge of k_{evap}, maximal dermal flux, and membrane lag time.

Introduction

Small quantities of chemicals come into contact with skin from both unintended exposures, such as splashes or contact with contaminated surfaces or even air, and intentional exposures such as the application of cosmetics, perfumes, and pharmaceutical formulations. Dermal risk assessment strategies require estimates of the uptake of such possibly harmful substances into the body. Uptake depends not only on mass loading and the area of contact but also on the interplay among kinetic variables including skin permeation rate, binding or chemical transformations within the skin, and evaporation from the skin surface. For neat liquids, evaporation reduces the amount that is absorbed, as some of the applied mass is lost to the surrounding environment. For volatile substances that do not undergo chemical transformations, current theory[1-4] provides sound theoretical estimates of the dermal uptake. For example, we have previously demonstrated[4] that knowledge of maximal steady-state dermal flux, lag time, and evaporation rate of the substance are sufficient to predict the eventual mass uptake from exposures to small or finite doses of a volatile chemical. While the first 2 variables are readily derived from *in vitro* experimental permeation experiments, knowledge of the evaporation rates of chemicals applicable to dermal exposures is limited.

Various experimental studies have reported measurements of evaporation rates of pools of volatile organic chemicals (VOCs), and mass transfer correlations have been derived and validated using these data[5-12]; (recently reviewed[13]). These correlations depend on physical properties of the liquid including vapor pressure and vapor diffusivity in air, as well as environmental factors such as wind velocity, temperature and pool size, and have found use, for example, in industrial processes and in the estimation of evaporation rates of environmental spills.

With notable exceptions, much less is known about the evaporation rates of thin films relevant to dermal exposures. Gajjar et al.[14] gravimetrically measured evaporation rates of 21 VOCs within walled *in vitro* diffusion cell caps. They tested the correlation of these data with several published mass transfer functions and proposed using one that was developed by the U.S. Environmental Protection Agency (EPA)[11] to estimate chemical spill evaporation rates. However, the general applicability of this or other mass transfer correlations to skin exposure settings has not been established. This knowledge gap constrains the rational application of quantitative dermal risk assessment strategies.

The authors declare no conflicts of interest to disclose.
This article contains supplementary material available from the authors by request or via the Internet at https://doi.org/10.1016/j.xphs.2018.04.020.

* *Correspondence to:* H. Frederick Frasch (Telephone: 304-285-5755).
E-mail address: HFrasch@cdc.gov (H.F. Frasch).

https://doi.org/10.1016/j.xphs.2018.04.020
0022-3549/

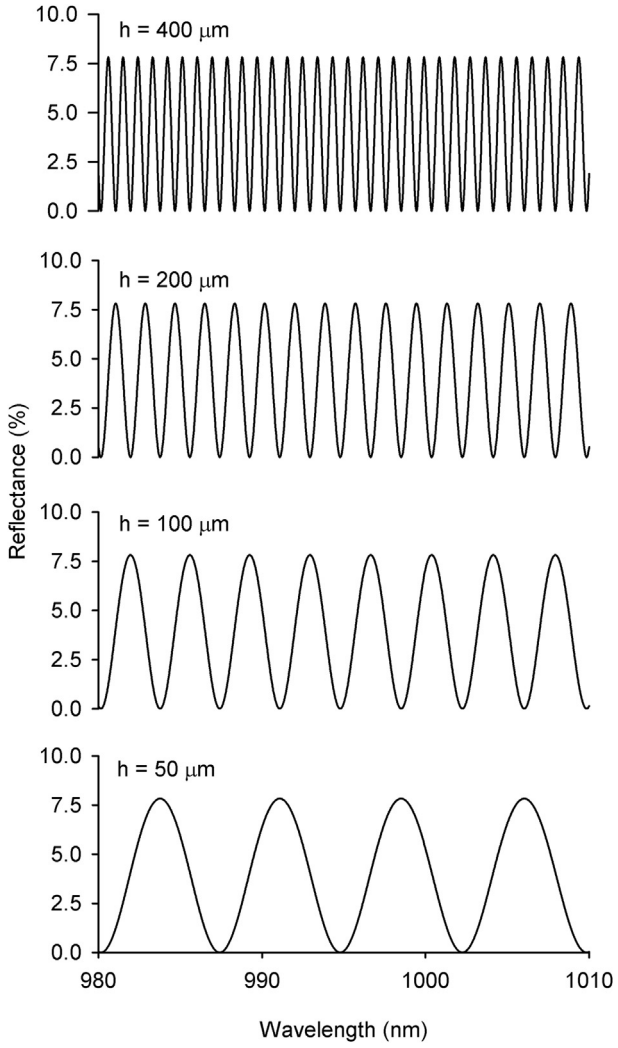

Figure 1. Theoretical optical reflectance of plane film of water surrounded by air, at listed thicknesses (h). Plots of Equation 2 with incident light angle = 0.

The aims of the current report are two-fold. First, we present the method of spectral reflectance as a tool to measure evaporation rates of thin (~25-300 μm) films of volatile neat organic chemicals. These data on 10 chemicals are compared with the predictions of a previously proposed[4] evaporative mass transfer coefficient. Second, we demonstrate an application of these data within an analytical framework to estimate the absorbed fraction of a semi-volatile neat chemical (nicotine) applied as a small dose on human skin *in vitro*.

Background and Theory

Spectral reflectance can quantify the thickness of a transparent liquid film. It measures reflected and/or transmitted light from a layered structure over a specified range of wavelengths and calculates the film thickness based on well-established optical theory. Consider the simple case of a plane parallel transparent film of thickness h and refractive index n_2, surrounded by a medium of refractive index n_1. A plane wave of monochromatic light, wavelength λ, is incident at an angle θ and is reflected off the inner surface of the film at angle θ'. It has been shown[15] that the phase difference δ between reflected waves from the inner and outer surfaces is related to the film thickness by:

$$\delta = \frac{4\pi}{\lambda} n_2 h \cos\theta' \tag{1}$$

and that the intensity of the reflected light I_r, normalized by incident intensity I_0, is given by

$$\frac{I_r}{I_0} = \frac{(2 - 2\cos\delta)R}{1 + R^2 - 2R\cos\delta} \tag{2}$$

where

$$R = \left(\frac{n_1 - n_2}{n_1 + n_2}\right)^2 \tag{3}$$

is the reflectivity of the film surface. Figure 1 displays Equation 2 for various thicknesses of water in air, with $\theta = \theta' = 0$. For films of these thicknesses, the curves appear near sinusoidal over a limited range of wavelengths, with multiple periods of very similar frequency. Thus, the fast Fourier transform (FFT) may be used to relate the fundamental frequency component to the film thickness. Similar theory applies to more complex layered structures, although analytical solutions such as Equation 2 may be elusive. The method has found broad applications in science and industry for coating and thin film analysis. It has been used to measure the thickness and sag of soap films,[16] but it has not, to our knowledge, been used to measure evaporation rates of VOCs.

The evaporation rate of a film within a constrained area can be determined from thickness measurements made over time. As outlined by Gajjar et al.,[14] the mass of an evaporating pool of pure liquid, initial mass M_0, on an impermeable surface is

$$m(t) = M_0 - m_{\text{evap}}(t), \tag{4}$$

with the evaporated mass given by

$$m_{\text{evap}}(t) = \int_0^t (k_{\text{evap}}\rho A)\,dt. \tag{5}$$

Here, ρ is the liquid density, A is the surface area of the pool, and k_{evap} (length/time) is a liquid-phase evaporation mass transfer coefficient. If these are constant over time, then

$$m(t) = M_0 - k_{\text{evap}}\rho A t, \tag{6}$$

and the area-normalized evaporative flux (mass/area/time) is:

$$J_{\text{evap}} = k_{\text{evap}}\rho. \tag{7}$$

Measurement of the thickness of the liquid film confined within a constant A over time represents a direct measurement of k_{evap}:

$$k_{\text{evap}} = -\frac{dh}{dt}. \tag{8}$$

To the extent that k_{evap} is constant over time and the area, $m(t)$ is readily determined.

An important parameter in mass transfer phenomena is the gas-phase mass transfer coefficient, k_g. The following relationship holds:

$$k_{\text{evap}}\rho = k_g \frac{p_{\text{vap}} MW}{RT}, \tag{9}$$

where p_{vap} is vapor pressure at the temperature of the liquid, MW represents molecular weight, T is liquid temperature, and R the gas constant. Various correlations have been published to estimate k_g

Table 1
Atomic and Structural Diffusion Volume Increments (Dimensionless) for Equation 13

Atom/Structure	Volume Increment
C	15.9
H	2.31
O	6.11
N	4.54
F	14.7
Cl	21.0
Br	21.9
I	29.8
S	22.9
Aromatic ring	−18.3
Heterocyclic ring	−18.3

Taken from Fuller et al[20].

based on physical properties and environmental conditions, hence measured evaporation rates may be compared with predictions from these correlations. Here, we correlate measured k_{evap} with predictions of a previously suggested[4] gas-phase mass transfer algorithm that is presented in mass transfer texts including Welty, Wicks and Wilson.[17] Assuming laminar flow parallel to a flat plate,

$$k_g = 0.664 D_{air}^{2/3} \left(\frac{u}{L}\right)^{1/2} \left(\frac{\rho_{air}}{\mu_{air}}\right)^{1/6}. \quad (10)$$

D_{air} is the chemical's diffusivity in air, u is wind speed, L is the square root of the application area, and ρ_{air} and μ_{air} are the density and viscosity of air, all in consistent units. The ratio μ_{air}/ρ_{air} is the kinematic viscosity of air which, at 760 Torr and 22°C, is 0.1532 cm^2/s.[18] Thus,

$$k_g = 3268 D_{air}^{2/3} \left(\frac{u}{L}\right)^{1/2}, \quad (11)$$

with k_g in cm/h, u in cm/s, L in cm, and D_{air} in cm^2/s.

When experimental data are unavailable, D_{air} for an evaporating chemical can be estimated from the correlation proposed by Fuller et al.:[19]

$$D_{air} = \frac{0.760 T_{air}^{1.75} [(MW + MW_{air})/(MW \cdot MW_{air})]^{1/2}}{P\left[(\sum v)^{1/3} + (\sum v)_{air}^{1/3}\right]^2} \quad (12)$$

with T_{air} in Kelvin and P (total pressure) in Torr (taken to be 760 Torr), MW is the molecular weight (g/mol) of the chemical, $MW_{air} = 29$, and the diffusion volume for air $(\Sigma v)_{air} = 19.7$. The sum of the volumes of molecular parts (Σv) for chemicals used here is calculated as

$$\left(\sum v\right) = 15.9 n_C + 2.31 n_H + 4.54 n_N + 6.11 n_O - 18.3 n_{ring} \quad (13)$$

where n_j is the number of parts of the molecule and j designates carbon (C), hydrogen (H), nitrogen (N), and oxygen(O) atoms or the number of aromatic or heterocyclic rings. These coefficient values were derived from experimental data correlations and reported in reference.[20] Estimated dimensionless volumetric contributions for these and other atoms, all derived from experimental data, are provided in Table 1.

With the assumption of laminar flow, Equation 10 in Equation 9 predicts that for a given exposure area, the evaporation rate will vary with the square root of wind speed. For turbulent flow, convective mass transfer theory[21] predicts an exponent value for wind speed dependency of $^4/_5$. Previously published k_g correlations span these extremes,[5-12] apparently reflecting the prevailing experimental conditions. The evaporation rate dependence on wind speed can readily be determined under controlled conditions.

Knowledge of the disposition of chemicals in contact with skin is of great interest in dermal risk assessment. For neat chemicals with some volatility, systemic uptake from dermal exposures to small doses will depend strongly on the evaporation rate of the chemical, as evaporation will decrease the mass of surface chemical available for permeation.

The mass of applied chemical that is absorbed over time is governed by a complex diffusion process that depends on skin and chemical properties and on environmental factors. Small or finite dose conditions, where the applied mass load is reduced through competing kinetic processes of surface evaporation and dermal absorption, are highly relevant to occupational, cosmetic, and pharmaceutical exposures. For finite doses of neat liquids, the dimensionless parameter χ, defined as the ratio of the evaporative flux to the maximal steady-state dermal absorption flux (J_{max}), is key:[1]

$$\chi = \frac{k_{evap}\rho}{J_{max}}. \quad (14)$$

Of primary interest in risk assessment is the total fraction of a small dose of chemical applied to the skin that is eventually absorbed into the body:

$$F_{abs} = \frac{M_{abs}}{M_0}. \quad (15)$$

Recent analyses that applied diffusion theory to a homogeneous membrane approximation of skin[3,4] presented strategies for calculating F_{abs} depending on specified boundary conditions. These estimates may be compared with the measured quantity to verify their applicability.

Methods

Chemicals

Chemicals were selected to span a broad range of vapor pressures, to have relevance in dermal risk assessment and to be liquids at experimental temperatures (21-32°C). Chemicals were used as purchased from Sigma-Aldrich, except as noted, with reported purities: methanol (99.9%; Fisher Chemical); ethanol (≥99.9%); 2-propanol (99.9%); 1-propanol (≥99.9%); isoamyl alcohol (~98%); nitrobenzene (99+%); 1-octanol (≥99%); (-)-nicotine (>99%); D-limonene (98%); and α-terpineol (≥96%).

Physical Properties

Table 2 presents relevant physical properties of the test chemicals. Liquid densities were taken from PubChem.[22] Refractive indices, measured at the He/Ne line (0.6328 μm) were taken from the refractive index database[23] except as indicated. Most vapor pressure data were taken from Perry's Chemical Engineers Handbook,[24] Table 2-8, which in turn was derived from the compilation of Stull.[25] The tabulated pressure−temperature data for each compound (10 pairs of values over the range of 1-760 torr) were subjected to regression analysis (SigmaPlot 13.0) to derive the parameter values A, B, and C of the Antoine equation

$$\log p_{vap} = A - \frac{B}{T + C} \quad (16)$$

to interpolate the values to the liquid test temperature T. For chemicals with p_{vap} <1 Torr, other data sources (cited in Table 2)

Table 2
Physical Properties, Derived, and Measured Values for Test Chemicals

Compound	Formula	*MW* (g/mol)	ρ (g/cm^3)	*n*	T_{air} (°C)	D_{air} (cm^2/s)	P_{vap} (Torr)	*u* (cm/s)	$k_{evap} \times 10^3$ (cm/h) Measured	$k_{evap} \times 10^3$ (cm/h) Predicted
Methanol	CH_4O	32.0	0.790	1.326	21.7	0.157	103	31.3 ± 0.4	1850 ± 101	1290
Ethanol	C_2H_6O	46.1	0.790	1.360	21.6	0.120	46.8	28.7 ± 0.4	558 ± 39	673
2-propanol	C_3H_8O	60.1	0.785	1.382	22.2	0.101	36.5	30.0 ± 0.7	834 ± 22	625
1-propanol	C_3H_8O	60.1	0.805	1.382	21.6	0.101	16.0	30.6 ± 0.7	306 ± 29	268
Isoamyl alcohol	$C_5H_{12}O$	88.2	0.810	1.406	22	0.0791	2.85	12.2	49.3	37.7
								12.5	45.9	38.1
								29.0	72.3	58.1
								30.4	72.9	59.4
								47.7	90.7	74.5
								98.8	126	107
								107	148	112
								162	178	137
								178	206	144
Nitrobenzene	$C_6H_5NO_2$	123.1	1.20	1.547	21.3	0.0783	0.215[a]	30.1 ± 0.6	4.73 ± 0.45	4.19
1-octanol	$C_8H_{18}O$	130.2	0.826	1.430[b]	21.5	0.0625	0.058[c]	28.1 ± 0.3	1.61 ± 0.24	1.44
Nicotine	$C_{10}H_{14}N_2$	162.2	1.01	1.528[b]	21.1	0.0630	0.029[d]	28.0 ± 1.5	0.867 ± 0.063	0.739
					22.0	0.0634	0.031[d]	114	1.65	1.59
d-limonene	$C_{10}H_{16}$	136.2	0.841	1.473[b]	21.7	0.0619	1.66	28.9 ± 0.7	42.5 ± 2.4	42.8
α-terpineol	$C_{10}H_{18}O$	154.3	0.935	1.483	21.2	0.0598	0.0427[e]	29.1 ± 1.6	1.25 ± 0.20	1.09

MW, molecular weight; ρ, liquid density; *n*: refractive index; T_{air}, measured air temperature (assumed equal to liquid temperature); D_{air}, diffusivity in air (calculated with Eqs. 12 and 13); p_{vap}, vapor pressure at liquid temperature; *u*, measured wind speed; k_{evap}, evaporation mass transfer coefficient measured and predicted from Equations 11-13 in Equation 9. *u* and measured k_{evap} values are mean ± SD from 3 replicates, except for isoamyl alcohol and a single nicotine experiment at $u = 114$ cm/h.

[a] Lynch EJ, Wilke CR 1960. Vapor pressure of liquid nitrobenzene at low temperatures. *J Chem Eng Data* 5: 300-300.

[b] *CRC Handbook of Chemistry and Physics*, 88th edition 2008. D R Lide, ed. Section 3-1, physical constants of organic compounds. CRC Press. p 3-1 − 3-523.

[c] NIST Chemistry Webbook. 1-octanol. http://webbook.nist.gov/cgi/cbook.cgi?ID=C111875&Mask=4&Type=ANTOINE&Plot=on.

[d] Banyasz, JL 1995. The physical chemistry of nicotine. In JW Gorrod and P Jacobs III, eds. *Analytical Determination of Nicotine and Related Compounds and their Metabolites*. Elsevier, Chapter 5, pp. 149-190.

[e] Li j, Perdue EM, Pavlosthathis SG, Araujo R 1998. Physicochemical properties of selected monoterpenes. *Environmental International* 24: 353-358. (Measured at 23.5°C).
Data sources: ρ: PubChem.[22] *n*: Refractive index database,[23] except where indicated. p_{vap}: Perry's Chemical Engineers Handbook,[24] except where indicated.

were used that included measurements at or near the relevant experimental temperatures.

For these studies, D_{air} were calculated by Equations 12 and 13 at the listed experimental temperatures, while k_g were calculated by Equation 11, that is, with $T_{air} = 295$ K (22°C), despite minor variations (±1°C) in experimental temperatures around this value. The resulting error is small, as the constant in Equation 11 ranges from 3277 to 3261 for temperatures between 20°C-25°C.

Evaporation Experiments

Film thickness measurements were made using a Filmetrics F3-S980 reflectance measurement system with thickness-solving software upgrade (Filmetrics Inc., San Diego, CA). Measurements were made over the wavelength range 980-1015 nm by focusing the normal incident light on the liquid sample with known refractive index. The sample holder was a 3 mm thick square (25 × 25 mm) smooth stainless steel plate with a 0.25 mm deep polished circular well 10 mm in diameter (0.79 cm^2). About, 20-30 μL of liquid (initial *h* 250-400 μm) was pipetted, and care was taken to ensure that the liquid was constrained within the confines of the circular area. Preliminary data for each chemical determined optimal focusing distance and total sampling time. Sampling time extended at least until half of the original thickness remained, but typically well beyond this point. Sample intervals from 2 s to 10 min were selected with the goal to capture at least 50 samples. The Filmetrics system estimates the thickness of the sample online by FFT of the reflectance data.

For these experiments, the instrument was placed within a crude wind tunnel constructed of heavy-duty aluminum foil that directed the output of a 7-inch circular 24V DC fan (SanAce M501) over the sample holder. The fan speed was controlled by a pulse width modulation system that also monitored wind speeds measured from a thin film anemometer (model 8455-03; TSI), placed 2 cm behind the sample holder with the transducer element in line with the sample. Measured wind speeds were consistent (SD <5% of the mean value) over the course of the experiment. No attempt was made to regulate the temperature of the evaporating liquid, which was assumed equal to the monitored room air temperature.

The mass transfer coefficient k_{evap} was determined at 21°C-22°C from the negative of the slope of the linear correlation with the data (*h* vs. time; Eq. 8). For all chemicals except isoamyl alcohol, 3 separate k_{evap} measurements were made, and mean and standard deviations were calculated. For these 9 chemicals, measurements reported here were performed at a target wind speed of 30 cm/s, selected as representative of indoor work places.[26] An additional measurement of nicotine at 114 cm/s was made. For isoamyl alcohol, 9 individual measurements were made over a range of *u* from 12.2 to 178 cm/s to examine the dependence of evaporation rate on wind speed. This chemical was selected simply for the convenience of its moderate vapor pressure, which enabled multiple k_{evap} determinations to be made within a day.

Skin Permeation Experiments

In vitro diffusion experiments were performed to measure the fraction of the total applied finite dose of nicotine that was absorbed through human epidermis. Details of the experimental method have been published elsewhere.[27] Heat separated human epidermal membranes (HEM) were used, derived from female breast reduction surgical material obtained following informed consent through Human Subjects Review Board—approved protocols from the West Virginia University tissue bank.

For the current experiments, modified Franz-type cells (PermeGear) were used (Fig. 2). These were 5 mL water-jacketed cells with 9-mm orifices (0.64 cm^2 exposure area), flat flange joints and "horseshoe" clamps. Modifications of the standard system were

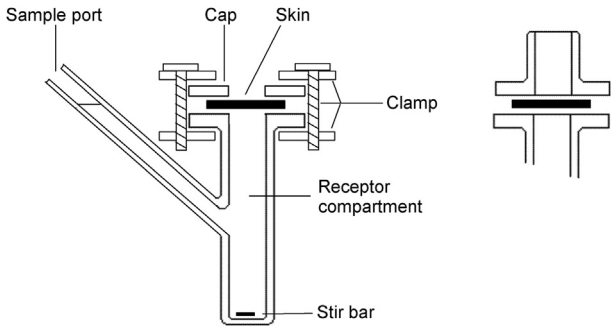

Figure 2. Modified Franz-type diffusion cell for human skin permeation studies. Donor formulation (5 μL/cm^2 nicotine) was applied to skin surface securely clamped to 5-mL receptor compartment using a 1.2-mm thickness type 316 stainless steel washer as cap. U-clamp surrounded skin on 3 sides, with open side facing the wind. Receptor fluid was stirred with magnetic bar, and samples (0.25 mL) are taken periodically through sample port. Not shown is the jacket surrounding the cell through which 37°C water was circulated, maintaining skin surface temperature of 32°C. At right, cut away shows standard diffusion cell cap with walled sides.

made to maximize skin surface exposure. First, the standard donor cell caps, with sides that protrude above the skin surface approximately 15 mm, were replaced by type 316 stainless steel washers, 1.2 mm thick, 25 mm diameter, with 10 mm orifices. Second, the horseshoe clamps were modified by inverting the clamps and replacing thumb screws with stainless steel pan head machine screws. The modified clamp plates extended 2.3 mm above the washers on 3 sides of the skin surface. The 2 screw heads protruded an additional 3 mm.

HEM samples (6 from the same human donor) were mounted on the cells the day before the experiment. Receptor fluid consisted of buffered (pH 7.4) Hank's balanced salt solution. The water-jacketed cells were maintained at 37°C, with skin surface temperature 32°C. The following morning, the 6-cell inline system was enshrouded within a heavy-duty aluminum foil "tunnel" which directed fan output of air at room temperature over the skin surfaces. Small access holes permitted sampling through the ports.

The applied donor formulation consisted of nicotine dissolved in acetone to deposit a load of 5 μL/cm^2 nicotine from a total application volume of 20 μL. Small-volume loads such as this are typical of workplace and cosmetic exposures and are recommended for dermal absorption study by international advisory authorities[28] but are difficult to spread evenly over the exposure area. Therefore, the nicotine was dissolved in a larger volume of acetone, which evaporates rapidly to leave a film of nicotine (initial h ~ 50 μm) over the skin surface. In our experience (unpublished results), exposures to this amount of acetone had no effect on HEM barrier function as assessed by transepidermal water flux.

Receptor solution was sampled (0.25 mL) at 0, 1, 2, 3, 4, 6, 8, 10, and 12 h and replaced with equal volumes of fresh buffer. Nicotine was quantified by HPLC.[27] Total mass absorption for each skin sample, taken as the cumulative nicotine mass in the receptor chamber and samples over time, was calculated from the sample concentrations. The applied nicotine masses were also quantified. Fractional absorption was calculated as absorbed mass at 12 h divided by the applied mass.

Results

Evaporation rate data were highly linear (R^2 ≥0.99), over the measured range, indicative of a constant k_{evap}. Measurements were repeatable, with the largest variance of 16% observed for α-terpineol. The spectral reflectance system exhibited no noticeable drift over time. Figure 3a presents thickness data of a film of nicotine exposed to 26.3 cm/s air speed over a time course of 25 h. As the film depletes (h <25 μm), a slower rate is observed which perhaps reflects additional interactive forces with the substrate as the film vanishes, reactions with air at the film surface, or perhaps changes in the velocity profile across the liquid surface as it dips well below the surface of the 250-μm-deep well. Linear regression (R^2 >0.999) gives k_{evap} = 8.781 × 10^{-3} cm/h (Eq. 8) and the standard error of the estimate = 2.163 × 10^{-6} cm/h. Figure 3b shows spectral reflectance % over the measured wavelength range for 3 data points, along with the calculated film thicknesses based on the FFT analysis.

Evaporation results for the 10 test chemicals are presented in Table 2. Nine chemicals were studied at similar u, but

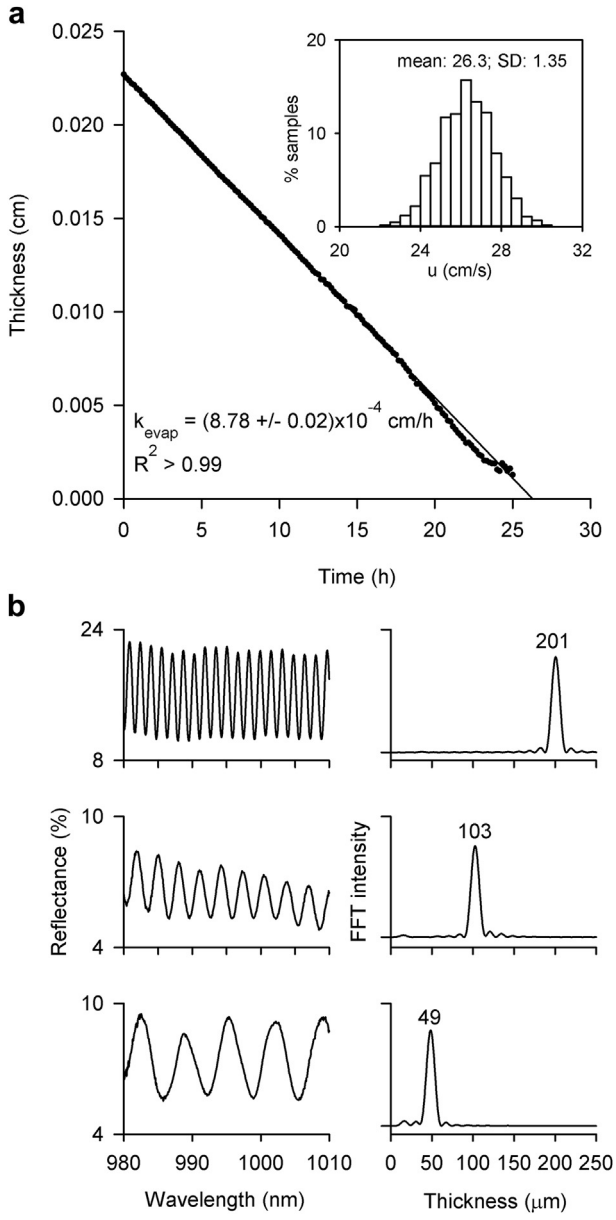

Figure 3. (a) Sequential thickness measurements of nicotine film over time. Solid line is the linear regression, which yields the slope (-8.78 × 10^{-4} cm/h) and standard error of the estimate (0.02 × 10^{-4} cm/h). The negative slope equals k_{evap}, the liquid-phase mass transfer coefficient. Inset: wind speed (u) measured over the time course of the thickness measurements. (b) Spectral reflectance and associated thickness determinations from FFT intensity for 3 of the data points.

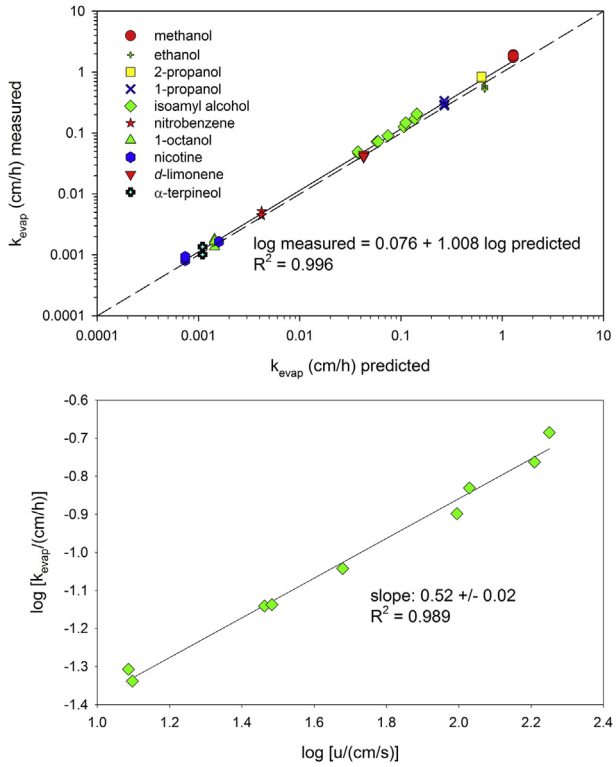

Figure 4. Top: Comparison of measured k_{evap} with predictions from Frasch and Bunge[4] (Eqs. 9 and 11-13). Dashed line is line of identity; solid line is linear regression. Bottom: Log-log plot of isoamyl alcohol k_{evap} with u gives the relationship $k_{evap} \propto u^{0.52}$, in good agreement with the prediction of Equations. 9 and 11: $k_{evap} \propto u^{1/2}$.

measurements of isoamyl alcohol were made over a range from 12.2 to 178 cm/s to investigate the dependence of k_{evap} on u.

The measured k_{evap} values were compared with predictions of Equation 9 using k_g calculated from Equations 11-13, and the comparison is shown in Figure 4. Correlation is excellent ($R^2 = 0.996$) for experimental values spanning over 3 orders of magnitude, and all data fall close to the line of identity. For isoamyl alcohol, the data demonstrate that $k_{evap} \propto u^{0.52}$, which compares quite favorably with the exponent value of ½ predicted by Equation 10. The scant data on nicotine also lends support, with k_{evap} measured at 28 and 114 cm/s consistent with a wind speed exponent of 0.46.

The skin permeation results are presented in Figure 5. The average absorbed mass reached a steady value by about 6 h, indicative of depletion of the applied mass. The absorbed mass at 12 h averaged 309 μg/cm^2 (SD = 119 μg/cm^2) from an applied load of 5014 μg/cm^2, for a fractional absorption of 0.062 ± 0.023. Wind speed measured over the diffusion cells was 36.2 ± 2.0 cm/s.

The value for fractional absorption is a key component in dermal risk assessment strategies. A recent analysis[4] that applied diffusion theory to a homogeneous membrane approximation of skin demonstrated how F_{abs} can be calculated based on the knowledge of k_{evap}, maximum dermal flux, and the membrane lag time. The calculations are straightforward but somewhat complicated, and the strategy is outlined in the Supplementary Material. Previous studies from our laboratory[27] report a mean ± SD maximum flux for nicotine of (175 ± 57) μg/cm^2/h and a lag time of (1.94 ± 0.72) h. Based on these mean values, estimates of F_{abs} were made. For this exercise, the mean measured k_{evap} value at 28.0 cm/s (8.67×10^{-4} cm/h) and the assumed liquid temperature of 21.1°C (Table 1) were modified to the experimental conditions (designated as′) of T' = 32°C (i.e., liquid temperature assumed equal to skin surface temperature) and measured u' of 36.3 cm/s, by using the relationships suggested by Equations 9 and 10, with T in Kelvin and $p_{vap}' = 0.072$ torr:

$$k'_{evap} = k_{evap}\left(\frac{u'}{u}\right)^{1/2}\left(\frac{p'_{vap}}{p_{vap}}\frac{T}{T'}\right) = 2.36 \times 10^{-3}\ \text{cm/h}. \quad (17)$$

Note that this adjustment makes the assumptions that the neat liquid density changes and air temperature differences are insignificant. Using this value of k_{evap}', the analysis outlined in the Supplementary Material predicts a value of $F_{abs} = 0.068$.

A different analysis[3] presented a simple equation for calculating F_{abs} under specified conditions:

$$F_{abs} = \frac{2 + f\chi}{2 + 2\chi}. \quad (18)$$

The variable f refers to the fraction of skin thickness (~0.1), consisting of loosely aggregated corneocytes that is readily accessible to the surface application of the chemical. Previous reports[1,3] should be consulted for additional details on the derivation and application of Equation 18. Using the mean experimental values and extrapolated estimate for k_{evap}' (Eq. 17),

$$\chi = \frac{k'_{evap}\rho}{J_{max}} = \frac{[2.36 \times 10^{-3}]\left(\frac{\text{cm}}{\text{h}}\right) \times [1.01 \times 10^{6}]\left(\frac{\mu\text{g}}{\text{cm}^3}\right)}{175\left(\frac{\mu\text{g}}{\text{cm}^2\text{h}}\right)} = 13.6; \quad (19)$$

$$F_{abs} = \frac{2 + 0.1\chi}{2 + 2\chi} = 0.115. \quad (20)$$

This value is higher than the previous estimate of 0.068, owing to different assumptions of the initial distribution of the applied load.

Discussion

The technique of spectral reflectance has been applied here for the systematic measurement of evaporation rates of thin films of volatile chemicals in the liquid state. The method has been shown

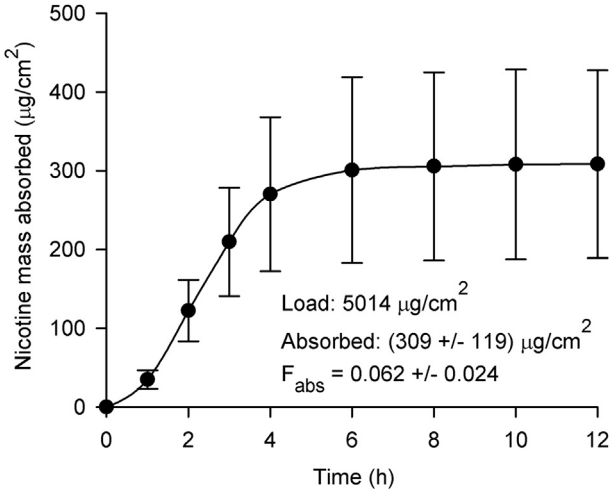

Figure 5. Plot of nicotine mass absorbed through human epidermis *in vitro* (mean ± SD, $n = 6$ samples from 1 individual) following exposure to 5 μL/cm^2. Solid lines are a guide to the eye. Fractional absorbed mass (F_{abs}) is calculated as the absorbed mass divided by the applied mass or load.

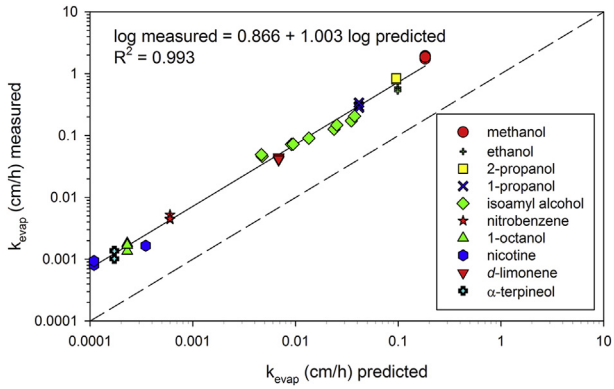

Figure 6. Correlation of measured k_{evap} with predictions of the EPA model (Eq. 21). Dashed line is line of identity; solid line is linear regression.

to be robust and repeatable, with evaporation rates that are constant over a broad range of film thicknesses. It is adaptable to stringent control of variables that affect evaporation rates including wind speed, liquid temperature, and surface area of exposure. In these experiments, we achieved good control of area and wind speed. The main limitation of these data was a lack of control of liquid temperature. Here, we assumed liquid temperature was identical to room temperature, which is adequate for slower-evaporating compounds but does not account for evaporative cooling which would lower the temperature (and hence vapor pressure) of the more volatile chemicals. Future endeavors will refine the wind tunnel, provide feedback control to more precisely lock in desired wind speeds, and will provide control of liquid temperature through a micro Peltier device within the sample holder. Realistic applications to dermal permeation may also have to consider the thermal conductivity of the skin as it relates to evaporative cooling.

The measured evaporation rates of 10 VOCs with vapor pressures spanning a 3500-fold range, correlate well with predictions of a previously suggested mass transfer coefficient given by Equation 10 (Fig. 4). Most measurements were made with similar wind speed of ~30 cm/s, but data from isoamyl alcohol measured over a range of u from 12.2 to 178 cm/s, as well as nicotine measured at 2 wind speeds, support the postulated square root dependence of k_{evap} on u. Data from additional chemicals will be required for a more definitive confirmation.

Most previous VOC evaporation measurements have been carried out in systems of larger size and higher wind speeds than would be applicable to skin exposures. By design, these studies have found applications to industrial processes and environmental remediation of large spills. A notable exception is the study of Gajjar et al.[14] The authors sought to measure and model k_{evap} in a system that is relevant to skin permeation experimental settings. They gravimetrically measured evaporation rates of 80 μL of 21 VOC's applied to glass or human skin surfaces constrained to 0.79 cm^2 area (~1 mm thick) by diffusion cell donor caps. Typically, these are walled glass caps that extend well above the membrane surface. Gajjar et al. measured evaporation rates on the laboratory bench top and in a fume hood. Their data set demonstrated excellent ($R^2 = 0.985$) correlation with a mass transfer coefficient advanced by the EPA for chemical spill evaluation[11]:

$$k_g = \frac{174u^{0.78}}{MW^{1/3}}, \tag{21}$$

with a parameter value u close to the air face velocity of their fume hood. However, it is important to recognize that wind speed was not measured; and therefore, the data do not permit verification of any particular velocity dependence. From our analysis (Supplementary Material in Frasch and Bunge[4]), we conclude that the data set is insufficiently robust to distinguish among competing mass transfer models. It is noteworthy that in the original study where the exponent value of 0.78 was proposed,[5] Mackay and Matsugu admit that "the effect of wind speed was impossible to separate from the other effects," and settled on the value of 0.78 as one that "seems appropriate." Thus, there is scant evidence to support this value.

A comparison of our data with well-defined u, with the EPA model Equation 21 shows (Fig. 6) consistent bias of underestimation of measured evaporation rates, by nearly an order of magnitude. Our studies were designed specifically to provide parallel air flow over the surface of the chemical itself. For this situation, flow is expected to be laminar for the exposed surface area and relevant wind speeds. The dimensionless Reynolds number Re, defined as

$$\mathrm{Re} = uL\rho_{air}/\mu_{air} \tag{22}$$

for flow across a smooth flat surface, is less than 10,000 for these studies, which is consistent with the observation that Equation 11 provides a superior fit with an air speed exponent value of ½. In this study, Re was ~200 for the diffusion cell experiments and between 200 and 1000 in the evaporation experiments. As a point of reference, for air at 22°C, $\mu_{air}/\rho_{air} = 0.1532$ cm^2/s, and flow parallel to a surface is expected to be laminar when $u \times L < 1532$ cm^2/s. Additional studies comparing k_{evap} from an open film and from within a walled diffusion cell cap are planned. Wind speed over the skin confined within typical walled diffusion cell caps would almost certainly be lower than in our system. The theory of diffusion through a stagnant gas film (refer to numerous sources including Welty et al.[29]) may be an appropriate analytical framework for the walled donor cap configuration.

For most realistic scenarios where chemicals come in contact with skin, the skin is directly exposed to the environment. (Exceptions include pharmacologic skin patch delivery systems and skin that is occluded by clothing.) Therefore, it seems appropriate to design *in vitro* studies to mimic closely the case where skin is open and not protected by the walls of a diffusion cell donor cap. This was the rationale for the modifications of the standard donor cap (Fig. 2). These modifications were not ideal in that the skin surface was still recessed below a 1.2-mm-thick washer, with additional U-clamp plates extending up on 3 sides. Owing to the requirement of a tight seal of the skin membrane to separate donor from receptor, it may be difficult to substantially improve on these simple modifications. These protrusions certainly altered the air stream over the skin surface compared with a fully open system, leading to uncertainty in local air flow variations in comparison with the measured bulk u.

Accurate k_{evap} values are crucial in the estimation of fractional absorption of chemicals applied as finite doses. For the nicotine study presented here, the mean F_{abs} was 0.062. Based on the measured k_{evap} modified in accordance with Equation 17 and previously reported nicotine J_{max} and τ, F_{abs} values of 0.068 and 0.115 were predicted (1.1- to 1.9-fold greater than the measured value). Considering the simplifications underlying the diffusion models, plus uncertainty in measured values and assumptions (local wind speed at skin surface; evaporation from skin instead of impermeable steel substrate; uncertainty of the distribution of the nicotine dose over the skin surface; and variances in measured J_{max} and τ values), this is a very good match. Absent consideration of chemical evaporation, the expected F_{abs} is 1. With no experimental data on k_{evap}, the predicted value from Equations 11-13 in Equation 9 gives an F_{abs} of 0.125 calculated by Equation 18. For comparison, the EPA model (Eq. 21 in Eq. 9) gives $F_{abs} = 0.385$.

Bekö et al.[30] estimated dermal uptake of nicotine from air *in vivo* of 1.53 μg/m^2 skin per μg/m^3 air concentration over a 5-h exposure. With a concentration of 250 μg/m^3 exposing a 2 m^2 human body, absorption of 765 μg of nicotine is estimated. This is comparable to a finite dose absorption of neat liquid nicotine over about 2.5 cm^2 of exposed skin (309 μg/cm^2 × 2.5 cm^2 = 772 μg). Clearly, both whole-body vapor exposure and limited-area dermal exposures to nicotine can result in nontrivial systemic nicotine uptake, comparable to quantities absorbed from smoking 1 cigarette.[27]

We have presented data that support a simple gas-phase mass transfer equation to estimate the evaporation rates of chemicals. We suggest that, in the absence of measured data, the analyses recommended herein be used for predicting fractional absorption of finite dose dermal exposures to neat liquids. Additional experiments are planned with other chemicals over a range of wind speeds to further address this conclusion. We reiterate that these results apply specifically to neat chemical liquid exposures. Additional systems of interest include volatile chemicals in nonvolatile vehicles, and volatile or nonvolatile chemicals in volatile vehicles. Results of this study are pertinent to these systems, although a more complex differential mass balance for the individual components will be required.

Acknowledgments

The findings and conclusions in this report are those of the authors and do not necessarily represent the official position of the National Institute for Occupational Safety and Health, Centers for Disease Control and Prevention. Financial support for this research was provided through intramural funding by the National Institute for Occupational Safety and Health. The research data used in preparation of the manuscript is available from the corresponding author.

References

1. Kasting GB, Miller MA. Kinetics of finite dose absorption through skin 2: volatile compounds. *J Pharm Sci*. 2006;95:268-280.
2. Anissimov YG. Mathematical models for different exposure conditions. In: Roberts MS, Walters KA, eds. *Dermal Absorption and Toxicity Assessment*. New York: Informa Healthcare; 2008:271-286.
3. Frasch HF. Dermal absorption of finite doses of volatile compounds. *J Pharm Sci*. 2012;101:2616-2619.
4. Frasch HF, Bunge AL. The transient dermal exposure II: post-exposure absorption and evaporation of volatile compounds. *J Pharm Sci*. 2015;104:1499-1507.
5. Mackay D, Matsugu RS. Evaporation rates of liquid hydrocarbon spills on land and water. *Can J Chem Eng*. 1973;1:434-439.
6. PACE Laboratories. *Evaporation Rate of Volatile Liquids*. Final Report, 2nd edition. EPA Contract number 68-DB-0112, Report number EPA/744-R-92-001. 1989.
7. Nielsen F, Olsen E, Fredenslund A. Prediction of isothermal evaporation rates of pure volatile organic compounds in occupational environments—a theoretical approach based on laminar boundary layer theory. *Ann Occup Hyg*. 1995;39:497-511.
8. Hummel AA, Braun KO, Feherenbacher MC. Evaporation of a liquid in a flowing airstream. *Am Ind Hyg Assoc J*. 1996;57:519-525.
9. Sparks LE, Tichenor BA, Chang J, Guo Z. Gas-phase mass transfer model for predicting volatile organic compound (VOC) emission rates from indoor pollution sources. *Indoor Air*. 1996;6:31-40.
10. Smith RL. Predicting evaporation rates and times for spills of chemical mixtures. *Ann Occup Hyg*. 2001;4:437-445.
11. Peress J. Estimate evaporative losses from spills. *Chem Eng Progr April*. 2003:32-34.
12. Heymes F, Aprin L, Bony A, Forestier S, Cirocchi S, Dusserre G. An experimental investigation of evaporation rates for different volatile organic compounds. *Process Saf Prog*. 2013;32:193-198.
13. Bubbico R, Mazzarotta B. Predicting evaporation rates from pools. *Chem Eng Trans*. 2016;48:49-54.
14. Gajjar RM, Miller MA, Kasting GB. Evaporation of volatile organic compounds from human skin *in vitro*. *Ann Occup Hyg*. 2013;57:853-865.
15. Born M, Wolf E. *Principles of Optics*. 4th ed. New York: Pergamon Press; 1970:323-329.
16. Huibers PDT, Shah DO. Multispectral determination of soap film thickness. *Langmuir*. 1997;13:5995-5998.
17. Welty JR, Wicks CE, Wilson RE. *Fundamentals of Momentum, Heat, and Mass Transfer*. 3rd ed. New York: John Wiley and Sons; 1984:595-601.
18. Wischnewski B. Calculation of thermodynamic states variables of air. Available at: http://www.peacesoftware.de/einigewerte/luft_e.html. Accessed March 1, 2018.
19. Fuller EN, Schettler PD, Giddings JC. A new method for prediction of binary gas-phase diffusion coefficients. *Ind Chem Eng*. 1966;58:19-27.
20. Fuller EN, Ensley K, Giddings JC. Diffusion of halogenated hydrocarbons in helium. The effect of structure on collision cross sections. *J Phys Chem*. 1969;73:3679-3685.
21. Welty JR, Wicks CE, Wilson RE. *Fundamentals of Momentum, Heat, and Mass Transfer*. 3rd ed. New York: John Wiley and Sons; 1984:603-606.
22. PubChem. Available at: https://pubchem.ncbi.nlm.nih.gov/. Accessed March 1, 2018.
23. Polyanskiy MN. Refractive index database. Available at: https://refractiveindex.info. Accessed March 1, 2018.
24. Perry RH, Green DW. *Perry's Chemical Engineering Handbook*. 7th ed. McGraw-Hill; 1999. Table 2-8. pp. 2-66—2-76.
25. Stull DR. Vapor pressure of pure substances. *Ind Eng Chem*. 1947;39:517-540.
26. Baldwin PEJ, Maynard AD. A survey of wind speeds in indoor workplaces. *Ann Occup Hyg*. 1998;42:303-313.
27. Frasch HF, Barbero AM. *In vitro* human epidermal permeation of nicotine from electronic cigarette refill liquids and implications for dermal exposure assessment. *J Expo Sci Env Epid*. 2017;27:618-624.
28. Organization for Economic Co-Operation and Development. OECD Guideline for the Testing of Chemicals. Test Guideline 428: Skin Absorption: In Vitro Method. Paris, France: OECD; 2004. Available at: http://www.oecd-ilibrary.org/environment/test-no-428-skin-absorption-in-vitro-method_9789264071087-en. Accessed March 1, 2018.
29. Welty JR, Wicks CE, Wilson RE. *Fundamentals of Momentum, Heat, and Mass Transfer*. 3rd ed. New York: John Wiley and Sons; 1984:524-526.
30. Bekö G, Morrison G, Weschler CJ, et al. Dermal uptake of nicotine from air and clothing: experimental verification. *Indoor Air*. 2017;28:247-257.